







Article

Mononuclear Fe(III) Schiff Base Complex with Trans-FeO₄N₂ Chromophore of *o*-Aminophenol Origin: Synthesis, Characterisation, Crystal Structure, and Spin State Investigation

Dawit Tesfaye ^{1,2,3,4} , Jonas Braun ⁵ , Mamo Gebrezgiabher ^{1,2} , Juraj Kuchár ⁴ , Juraj Černák ⁴, Taju Sani ^{1,2} , Abbasher Gismelseed ⁶ , Tim Hochdörffer ⁷, Volker Schünemann ⁷, Christopher E. Anson ⁵ , Annie K. Powell ^{5,*}  and Madhu Thomas ^{1,2,*} 

- ¹ Department of Industrial Chemistry, College of Natural and Applied Sciences, Addis Ababa Science and Technology University, Addis Ababa P.O. Box 16417, Ethiopia; dawit.tesfaye@aastu.edu.et (D.T.); mamo.gebrezgiabher@aastu.edu.et (M.G.); taju.sani@aastu.edu.et (T.S.)
 - ² Nanotechnology Center of Excellence, Addis Ababa Science and Technology University, Addis Ababa P.O. Box 16417, Ethiopia
 - ³ Department of Chemistry, College of Natural Sciences, Salale University, Fitche P.O. Box 245, Ethiopia
 - ⁴ Department of Inorganic Chemistry, Institute of Chemistry, P. J. Šafárik University in Košice, Moyzesova 11, 041 54 Košice, Slovakia; juraj.kuchar@upjs.sk (J.K.); juraj.cernak@upjs.sk (J.Č.)
 - ⁵ Institute of Inorganic Chemistry (AOC), Institute of Nanotechnology (INT) and Institute for Quantum Materials and Technologies (IQMT), Karlsruhe Institute of Technology (KIT), Kaiserstr. 12, 76131 Karlsruhe, Germany; jonas.braun2@kit.edu (J.B.); christopher.anson@kit.edu (C.E.A.)
 - ⁶ Department of Physics, College of Science, Sultan Qaboos University, Al-Khod P.O. Box 36, Oman; abbasher@squ.edu.om
 - ⁷ Department of Physics, University of Kaiserslautern-Landau, Erwin-Schrödinger-Strasse 46, 67663 Kaiserslautern, Germany; hochdoer@rhrk.uni-kl.de (T.H.); schuene@physik.uni-kl.de (V.S.)
- * Correspondence: annie.powell@kit.edu (A.K.P.); madhu.thomas@aastu.edu.et (M.T.)



Citation: Tesfaye, D.; Braun, J.; Gebrezgiabher, M.; Kuchár, J.; Černák, J.; Sani, T.; Gismelseed, A.; Hochdörffer, T.; Schünemann, V.; Anson, C.E.; et al. Mononuclear Fe(III) Schiff Base Complex with Trans-FeO₄N₂ Chromophore of *o*-Aminophenol Origin: Synthesis, Characterisation, Crystal Structure, and Spin State Investigation. *Inorganics* **2024**, *12*, 159. <https://doi.org/10.3390/inorganics12060159>

Academic Editor: Isabel Correia

Received: 14 May 2024

Revised: 28 May 2024

Accepted: 29 May 2024

Published: 3 June 2024



Copyright: © 2024 by the authors. Licensee MDPI, Basel, Switzerland. This article is an open access article distributed under the terms and conditions of the Creative Commons Attribution (CC BY) license (<https://creativecommons.org/licenses/by/4.0/>).

Abstract: A new iron(III) complex (Et₃NH)₂[Fe(L)₂](ClO₄)·MeOH (1) where H₂L = 2-[(E)-[2-hydroxyphenyl]imino]methyl]phenol has been synthesised and characterised by single crystal XRD, elemental analysis and DC magnetic susceptibility measurements. The dianionic ligands L²⁻ coordinate in a tridentate fashion with the Fe(III) through their deprotonated phenolic oxygens and azomethine nitrogen atoms, resulting in a trans-FeO₄N₂ chromophore. Variable-temperature magnetic measurements were performed between 300 and 5 K under an applied field of 0.1 T and show that 1 is in the high spin state (S = 5/2) over the whole measured temperature range. This is confirmed by Mössbauer spectroscopy at 77 and 300 K.

Keywords: iron(III); Schiff base; complex; spin state; Mössbauer spectroscopy

1. Introduction

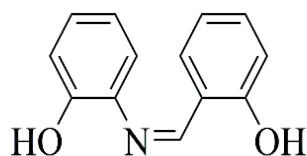
The design and synthesis of a particular ligand field are crucial factors in generating coordination compounds with desired properties. Schiff base ligands have drawn much attention due to their ease in bringing the required coordination sites together by a simple imine condensation reaction [1] and their complexes have been involved in catalysis and enzymatic reactions [2–6] magnetic studies and molecular architectures [7,8].

With respect to magnetically interesting systems, Schiff base complexes with a six-coordinate environment with N₆ and N₄O₂ coordination for Fe(II) or N₄O₂, N₂S₂O₂, and S₆ coordination for Fe(III) may lead to the generation of spin crossover compounds [9]. In this paper, we have employed a Schiff base ligand, formed by condensing *o*-aminophenol and salicylaldehyde, which can chelate Fe(III), generate an octahedral geometry with a N₂O₄ coordination environment, and have investigated its spin state.

There are few reports in the recent literature on the synthesis, characterisation, and magnetic properties of N₂O₄-coordinated Fe(III) complexes with a Schiff base formed from

o-aminophenol and salicylaldehyde [10–12]. Such N_2O_4 -Fe(III) complexes are reported [9] to show a wide range of magnetic behaviours, including high spin, low spin, and SCO behaviour, depending on the fine tuning of the ligand field. It is interesting to note that many of these types of complexes have a counter cation along with the counter anions to balance the overall charge [10–12]. In the complexes mentioned above, the significance of the *o*-aminophenol moiety is the possibility of chelation. This can occur as part of a larger Schiff base ligand, as in the present case, or in its original form. The biological and spectroscopic relevance of this moiety was highlighted in an insightful review by Abdallah et al. [13], and the use of it as a feedstock for oxidation catalysis was summarised by Jana et al. [14].

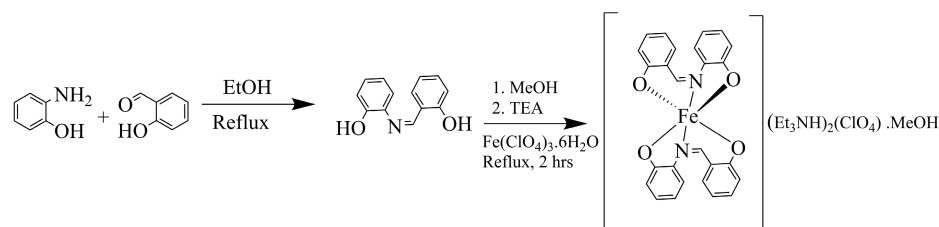
As part of our ongoing interest in SCO Schiff base iron complexes and their spin states [15–19], we report here our investigations on the structure and spin state of an iron(III) complex with the doubly deprotonated form of the proligand 2-((E)-[2-hydroxyphenyl]imino)methylphenol (H_2L) (Scheme 1). The ligand L^{2-} coordinates in a tridentate chelating mode through the two deprotonated phenolate oxygens and the azomethine nitrogen. The +3 oxidation state of iron is balanced by two protonated triethylammonium cations as well as a perchlorate anion. The complex remains in a HS condition throughout the measured temperature range of 5–300 K. This is supported by Mössbauer spectra performed at 77 and 300 K, which are influenced by paramagnetic relaxation effects.



Scheme 1. Schematic representation of the Schiff base 2-((E)-[2-hydroxyphenyl]imino)methylphenol (H_2L).

2. Results and Discussion

The synthesis of the ligand and complex is displayed in Scheme 2.



Scheme 2. Reaction scheme leading to product 1.

2.1. Crystal Structure

The crystal structure of **1**, $(Et_3NH)_2[Fe(L)_2](ClO_4) \cdot MeOH$ is ionic and consists of two $(Et_3NH)^+$ cations, one complex $[Fe(L)_2]^-$ anion, one ClO_4^- anion, and one solvent molecule of methanol. The central Fe(III) is coordinated by two tridentate dianionic ligands, L^{2-} , formed from the doubly deprotonated Schiff base H_2L (Scheme 2, Figure 1).

A search in the CSD [20] has shown that the crystal structure of the Schiff base H_2L has been reported four times at RT, of which the best refinement appears to be that of Tunc et al. [21]. An additional search in the CSD shows that the title complex is novel, although the mononuclear complex anion has previously been reported with a range of counterions and/or solvents: $K[Fe(L)_2] \cdot MeOH$ [10], $(NH_4)[Fe(L)_2] \cdot H_2O$ [11], $(Me_4N)[Fe(L)_2]$ [12], $K[Fe(L)_2] \cdot H_2O$ [22], $(Pr_3NH)[Fe(L)_2] \cdot 2CH_3OH$ [22], $[Fe(L)(bpyO_2)(CH_3OH)][Fe(L)_2] \cdot MeOH$ [22], and $[Fe(L)(HL)]_2$ [23]. In addition to this, a polynuclear Fe_4 propeller-type complex $[Fe_4(L)_6] \cdot 2(CH_3)_2CO$ has been reported with the same ligand system, in which the iron ions are bridged by deprotonated hydroxy groups of the ligands [10].

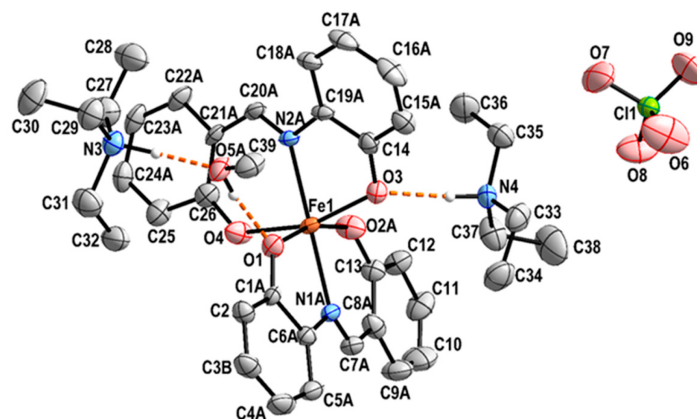


Figure 1. View of the structure of complex **1** along with the atom numbering scheme. Hydrogen bonds are shown as dashed orange lines. Hydrogen atoms bonded to carbon are omitted for clarity. For the sake of clarity, only atoms with higher occupation factors are shown. The thermal ellipsoids are drawn at a 30% probability level.

Various synthetic protocols have been adopted to target the complexes mentioned above. In most cases, a base was employed, facilitating the deprotonation of the Schiff base ligand and simultaneously balancing the charge of the complexes by counterion formation.

Among the mentioned complexes, $K[Fe(L)_2] \cdot MeOH$ [10] and $(NH_4)[Fe(L)_2] \cdot H_2O$ [11] were synthesised by reacting the metal salt and ligand in non-aqueous solvents with the corresponding bases, with only $[Fe(L)(HL)]_2$ [23] accessible without base. $(Me_4N)[Fe(L)_2]$ [12] was synthesised from the complex precursor $K[Fe(azp)_2] \cdot MeOH \cdot (C_2H_5)_2O$ in the presence of the base trimethyl amine. It is interesting to note that $K[Fe(L)_2] \cdot H_2O$ and $(Pr_3NH)[Fe(L)_2] \cdot 2CH_3OH$ [22] was generated in situ by mixing the individual components in one pot. In addition to this, $[Fe(L)(bpyO_2)(CH_3OH)][Fe(L)_2] \cdot MeOH$ [22] was synthesised from the respective complex entities in methanolic medium.

It is worth noting that the synthetic procedure we report in the present article is consistent with the synthetic protocols mentioned above.

In the present complex, the central Fe(III) exhibits a rather distorted octahedral $trans-FeO_4N_2$ coordination environment (Figure 1). The two tridentate chelating ligands are coordinated in a *mer*-fashion. It should be noted that both anionic ligands L^{2-} are positionally disordered (Figure 2). A similar disorder has been previously observed [22]. The SHAPE analysis [24] shows that the Fe(III) coordination environment is best described as a distorted octahedron (Table S1).

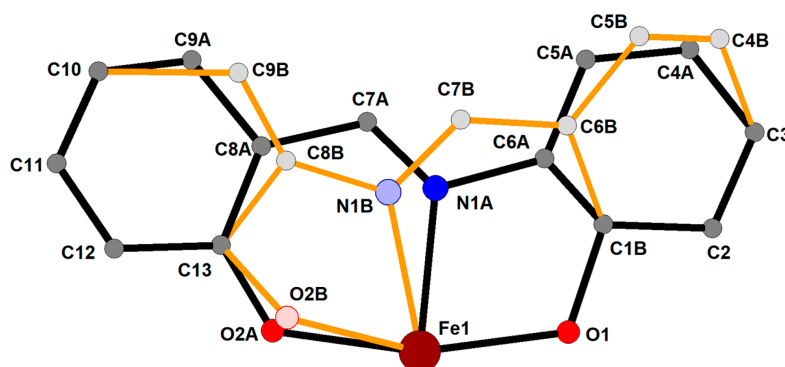


Figure 2. View on the positional disorder of the ligand L^{2-} -coordinating the Fe(III) central atom. Only one ligand is shown for clarity; the second ligand displays the same type of disorder. The site occupation factors for the two disordered positions A and B are 0.777(3) and 0.223(3), respectively. Hydrogen atoms are omitted.

The Fe-O and Fe-N bond distances (Table 1) are in the ranges 1.957(2)–2.031(2) Å and 2.076(19)–2.140(4) Å, respectively. These compare well with the corresponding distances in the previously reported compounds [22,23]. The negative charges of the perchlorate anion and of the complex anion are counterbalanced by the positive charges of two crystallographically independent (Et₃NH)⁺ cations.

The methanol solvate molecule is involved in two rather strong hydrogen bonds. The OH...O type hydrogen bond links the methanol molecule to the complex anion via O1 acting as acceptor, while the methanol oxygen itself accepts a hydrogen bond of the N-H...O type from the triethylammonium nitrogen atom N3. The second triethylammonium cation forms a N-H...O hydrogen bond from N4 to O3 of the complex anion (Figures 1 and 3, Table 2).

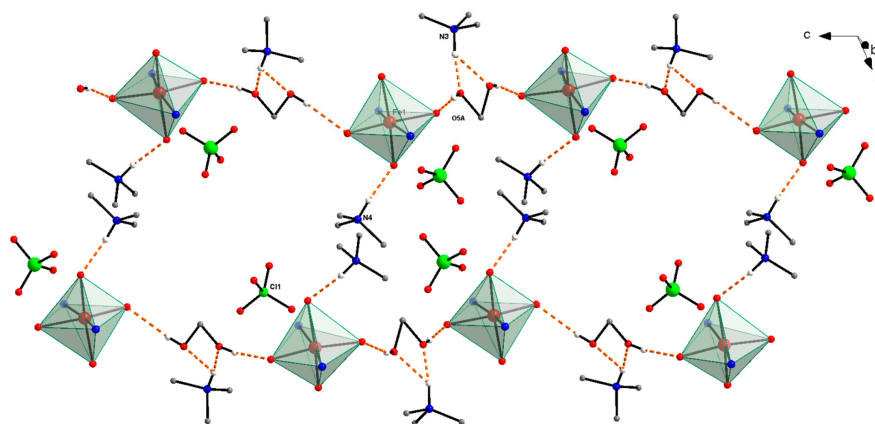


Figure 3. Packing view of the crystal structure of **1**. For the sake of clarity, the complex anions are represented only by coordination polyhedral, and from tetraethylammonium cations, only the carbon atoms bonded to the nitrogen atoms are shown. All hydrogen atoms not involved in hydrogen bonds (shown as dashed orange lines) are also omitted.

Table 1. Selected geometric parameters [Å, °] in **1** and comparison with the same parameters in selected analogous complexes [22,23].

Complex 1 (170 K)	(Pr ₃ NH)[Fe(L) ₂] (150 K) [22]	[Fe(L)(HL)] ₂ (150 K) [23]
Fe1-O1 1.988(2)	1.9851(19)	2.078(2) 2.091(2)
Fe1-O2A 1.963(5)	1.947(2)	1.926(2) 1.915(2)
Fe1-O3 2.031(2)	2.004(2)	2.083(2) 2.067(2)
Fe1-O4 1.958(2)	1.948(2)	1.912(2) 1.919(2)
Fe1-N1A 2.144(4)	2.117(5)	2.108(3) 2.133(2)
Fe1-N2A 2.139(4)	2.167(4)	2.105(2) 2.127(3)
O1-Fe1-N1A 76.70(12)	75.75(12)	77.69(8) 76.36(8)
O2A-Fe1-N1A 87.85(19)	89.79(12)	88.39(9) 86.75(9)
O3-Fe1-N2A 75.99(12)	72.00(13)	77.53(9) 76.68(9)
O4-Fe1-N2A 85.89(13)	90.18(14)	88.13(9) 87.05(9)
O1-Fe1-O2A 164.43(17)	163.68(9)	164.13(8) 159.80(8)
O4-Fe1-O3 161.85(11)	161.80(10)	164.00(8) 161.23(9)

Table 2. Hydrogen bonds in **1** [Å, °].

D-H...A	D-H	D...A	H...A	DHA
O5A-H5A1...O1	0.84	1.85	2.386(4)	173
N3-H1N3...O5A	1.07	1.66	2.720(5)	173
N3-H1N3...O5B	1.07	2.02	2.804(14)	127
N4-H1N4...O3	0.92	1.88	2.796(4)	173
N4-H1N4...O2B	0.92	2.57	3.023(3)	122

2.2. Magnetic Properties

The magnetic susceptibility measurements of the complex $(\text{Et}_3\text{NH})_2[\text{Fe}(\text{L})_2](\text{ClO}_4)\cdot\text{MeOH}$ were recorded in both heating (\uparrow) and cooling cycles (\downarrow) in the temperature range 5–300 K in an MPMS3 SQUID magnetometer at two different temperature scan rates of 3 K/min and 5 K/min using an applied magnetic field of 0.1 T. The $\chi_{\text{M}}T$ vs. T plot is shown in Figure S2. The room-temperature $\chi_{\text{M}}T$ value of the complex is $4.95 \text{ cm}^3 \text{ K mol}^{-1}$, consistent with the HS state. On decreasing the temperature, the $\chi_{\text{M}}T$ value decreases slightly to reach a minimum of $4.5 \text{ cm}^3 \text{ K mol}^{-1}$ at 5 K, confirming that the compound is locked in the HS condition throughout the measured temperature range of 5–300 K. An N_2O_4 environment is usually considered to be a weak ligand field for Fe(III), and such complexes are expected to be in the HS state [12].

2.3. Mössbauer Spectroscopy

The Mössbauer spectrum of compound **1** obtained at 77 K is shown in Figure 4a. The spectrum has an isomer shift $\delta = 0.50 \text{ mm s}^{-1}$, which is characteristic for Fe(III) in its high spin $S = 5/2$ state [25]. The spectrum is broadened because of the magnetic relaxation of the $S = 5/2$ system. Such effects happen when the electronic spin relaxation time is comparable to the Larmor frequency of the ^{57}Fe nucleus in the magnetic hyperfine field of the iron atom, which can be up to 55 T in $S = 5/2$ systems. Raising the temperature to 300 K still leads to significant magnetic broadening in the Mössbauer spectrum (Figure 4b). Such nearly-temperature-independent behaviour is typical for spin-spin relaxation processes [26]. The fact that the isomer shift decreases to 0.40 mms^{-1} at 300 K is due to a second-order Doppler shift effect. In conclusion, Mössbauer spectroscopy confirms that compound **1** is a ferric high-spin system independent of temperature.

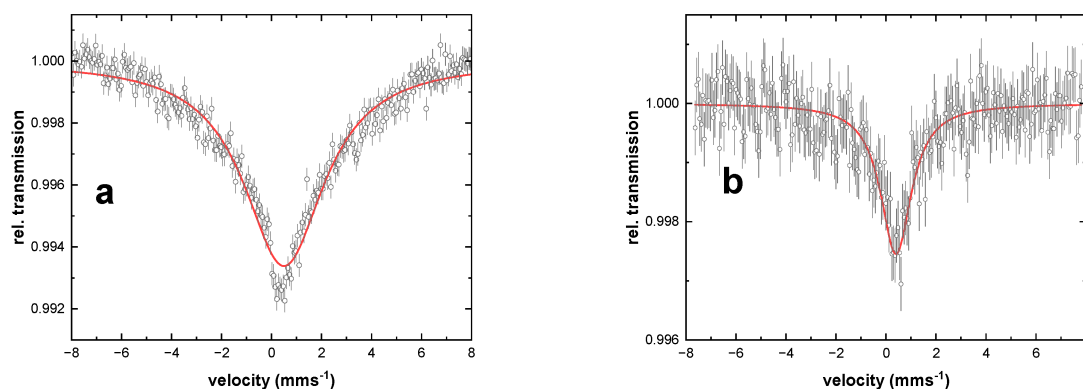


Figure 4. Mössbauer spectra of **1** at (a) 77 K and (b) 300 K. The open circles and error bars show the experimental data, and the red solid lines are from simulations with the parameters given in Table 3.

Table 3. Mössbauer parameters of compound **1** as obtained from the analysis displayed in Figure 4. The data has been analysed with a doublet having Lorentzian line shape with full width at half maximum Γ . The red lines in Figure 4 are the results of free fits which resulted in artificially large values of Γ due to electronic relaxation effects.

	77 K	300 K
δ (mms^{-1})	0.50(4)	0.40(5)
ΔE_{Q} (mms^{-1})	0.00(5)	0.00(5)
Γ (mms^{-1})	4.50(30)	1.50(30)

3. Experimental Section

3.1. Materials and Methods

All chemicals and reagents were purchased from commercial sources and were of analytical reagent grade. They were used without further purification except for ethanol,

which was purified by standard methods. FTIR spectra were measured in the range on a PerkinElmer FTIR spectrometer (Wellesley, MA, USA). Elemental analyses were carried out on an Elementar Vario MicroCube (Elementar Analysensysteme, Langensfeld, Germany). Single crystal XRD measurements were performed with Xcalibur Oxford Diffraction (Rigaku) diffractometer (Oxford Diffraction Limited, Oxfordshire, UK). Magnetic susceptibility measurements were carried out on an MPMS-3 SQUID magnetometer (Quantum Design GmbH, Pfungstadt, Germany) operating between 5 and 300 K with an applied magnetic field of 0.1 T. Mössbauer spectra were recorded using a ^{57}Co source in transmission geometry in the time-scale mode in conjunction with a 512-channel analyzer (WissEl GmbH, Starnberg, Germany). Variable temperature experiments were performed using a continuous flow cryostat (OptistatDN, Oxford Instruments, Abingdon, UK). The spectrometer was calibrated against $\alpha\text{-Fe}$ at room temperature, and analysis of the spectral data was performed using the public domain programme Vinda running on Excel 2003[®] platform with least-squares fits of Lorentzian line shapes [27].

3.2. Synthesis

3.2.1. Synthesis of the Ligand 2-((E)-[2-hydroxyphenyl]imino)methylphenol (H_2L)

The tridentate Schiff base H_2L = 2-((E)-[2-hydroxyphenyl]imino)methylphenol was prepared by the reported procedure [21].

3.2.2. Synthesis of the Complex $(\text{Et}_3\text{NH})_2[\text{Fe}(\text{L})_2](\text{ClO}_4)\cdot\text{MeOH}$ (1)

To a stirred solution of H_2L (0.106 g, 0.5 mmol) in methanol (20 mL), was added triethylamine (0.1 g, 1 mmol) and further stirred for half an hour. $\text{Fe}(\text{ClO}_4)_3\cdot 6\text{H}_2\text{O}$ (0.0885 g, 0.25 mmol) was added to the resultant solution and refluxed for 2 h. The brown solution obtained was allowed to cool and then filtered. Slow vapour diffusion of diethyl ether into the filtrate gave black needle-like crystals suitable for X-ray diffraction measurements. Yield: 47% (0.091 g): Anal. $\text{C}_{39}\text{H}_{54}\text{FeN}_4\text{O}_9\text{Cl}$. Calcd. C, 57.53; H, 6.69; N, 6.88%; Found C, 57.39; H, 6.56; N, 7.01% FT-IR (cm^{-1}): 3440 (s), 1603 (s), 1532 (m), 1465 (s), 1385 (m), 1297 (m), 1118 (s), 921 (w), 830 (m), 758 (m), 622 (w), 522 (m) (Figure S1).

Caution! Perchlorate salts of metal complexes with organic ligands are potentially explosive and should be handled in small quantities with care.

3.3. Single Crystal Structure Analysis

X-ray diffraction data were collected at 173(2) K on an Xcalibur Oxford Diffraction (Rigaku) diffractometer equipped with a Sapphire2 detector and graphite-monochromated Mo- $\text{K}\alpha$ radiation ($\lambda = 0.71073 \text{ \AA}$) using the CrysAlisPro software (Version 1.171.41.93a) [28]. The data were corrected for absorption using numerical absorption correction based on gaussian integration over a multifaceted crystal model, with $T_{\text{min}} = 0.813$ and $T_{\text{max}} = 0.931$. The structure was solved by direct methods and refined by full-matrix least-squares techniques on F^2 using programmemes SHELXT and SHELXL [29,30], which were incorporated in the WinGX programme package (<https://journals.iucr.org/paper?S0021889812029111>) [31]. All non-hydrogen atoms, including the disordered atoms of the ligands (common thermal ellipsoids were used for the same atom in the two disordered positions), were refined with anisotropic thermal parameters. Organic hydrogen atoms on the ligands and counteractions were placed in calculated positions with a riding model. The positional coordinates of the hydroxyl hydrogen atoms in the methanol (C39A/C39B, O5A/O5B atoms) solvate molecule were treated as idealised hydroxyl groups. During the refinement process, it became clear that both chelating L ligands show head-to-tail positional disorder. The disorder was modelled using the distinct positions of several atoms of L. Their site occupation factors were refined, and the final values were 0.777(3) for the major component (labelled with A) and 0.223(3) for the minor one (B). The thermal parameters of the disordered atoms were treated with common thermal motion using EADP commands. Structural figures were drawn using Diamond [32]. Crystal data and refinement results for the complex are summarised in Table 4, and the selected bond lengths and bond angles of the complex are presented in Table 1.

Table 4. Crystal data and structure refinement for Complex 1.

Empirical formula	C ₃₉ H ₅₄ ClFeN ₄ O ₉
Formula weight	814.16
Temperature	173(2) K
Wavelength	0.71073 Å
Crystal system, space group	Monoclinic, P2 ₁ /c
Unit cell dimensions [Å, °]	a = 17.0219(6) α = 90 b = 15.1654(3) β = 117.540(4) c = 17.7368(6) γ = 90
Volume [Å ³]	4059.8(3)
Z, Calculated density [Mg/m ³]	4, 1.332
Absorption coefficient	0.495
F(000)	1724
Crystal size [mm]	0.578 × 0.343 × 0.199
θ range for data collection [°]	2.918 to 26.000
Limiting indices	−20 ≤ h ≤ 20, −18 ≤ k ≤ 18, −20 ≤ l ≤ 21
Reflections collected / unique	41,409/7954 [R(int) = 0.0247]
Completeness to θ = 26.000	99.8 %
Absorption correction	Analytical
Max. and min. transmission	0.931 and 0.813
Refinement method	Full-matrix least-squares on F ²
Data / restraints / parameters	7954/0/566
Goodness-of-fit on F ²	1.044
Final R indices [I > 2σ(I)]	R1 = 0.0631, wR2 = 0.1717
R indices (all data)	R1 = 0.0783, wR2 = 0.1830
Largest diff. peak and hole [e.Å ^{−3}]	0.972 and −0.506

4. Conclusions

In summary, an Fe(III) complex with a tridentate Schiff base ligand derived from *o*-aminophenol and salicylaldehyde (H₂L) has been synthesised and characterised by elemental analysis, FTIR, single crystal XRD, magnetic susceptibility measurements and Mössbauer spectroscopy. The ligand coordinates with the central metal ion through both the deprotonated phenolate oxygen and azomethine nitrogen. Two ligand molecules chelate the central metal ion, leading to a distorted octahedral geometry with two protonated triethylammonium counteranions along with a perchlorate counteranion to balance the charge. Variable-temperature magnetic measurements prove that the compound is locked in its HS state over the whole measured temperature range (300–5 K), while Mössbauer measurements at 77 and 300 K reveal paramagnetic relaxation effects.

Supplementary Materials: The following supporting information can be downloaded at: <https://www.mdpi.com/article/10.3390/inorganics12060159/s1>; Figure S1: FT-IR spectra of Complex (Et₃NH)₂[Fe(L)₂](ClO₄)·MeOH; Figure S2: X_MT vs. T curve for the complex (Et₃NH)₂[Fe(L)₂](ClO₄)·MeOH. Figure S3: ESI-MS of (Et₃NH)₂[Fe(L)₂](ClO₄)·MeOH measured in negative-ion mode. The 100% peak corresponds to the monoanionic complex. Figure S4: ESI-MS of (Et₃NH)₂[Fe(L)₂](ClO₄)·MeOH measured in positive-ion mode. Table S1: The geometry of coordination polyhedrons was calculated in the SHAPE v2.1 program.

Author Contributions: The major work for this article—designing, execution, and writing of the original draft as part of his Ph.D. programme—was done by the first author (D.T.). The second author (J.B.) has participated in characterisation (SQUID measurement) as well as editing and reviewing this article. The third author (M.G.) has participated in formal analysis, co-investigation, writing, and editing. The fourth and fifth authors, J.K. and J.Č., were responsible for solving the crystal structure, analysis, and writing, as well as funding acquisition. The sixth author (T.S.) was participated in data curation. The other authors (A.G., T.H. and V.S.), were responsible for Mössbauer measurement, analysis, editing, and reviewing of this article. In addition, the authors (J.Č., C.E.A., A.K.P. and M.T.) were responsible for the supervision, editing, and reviewing of this article. All authors have read and agreed to the published version of the manuscript.

Funding: This work was supported by the Scientific Grant Agency of the Ministry of Education, Science, Research and Sport of the Slovak Republic (contract No. VEGA 1/0189/22) (J.C. and J.K.), German Ministry of Research (BMBF) under 05K22UK1 (V.S), Helmholtz Foundation POF MSE (J.B., C.E.A. and A.K.P.), and internal research grants (IG 07/2021 and IRG 08/2024) (M.T. and M.G.), of Addis Ababa Science and Technology University.

Data Availability Statement: CCDC number 2344025 contain the supplementary crystallographic data for this paper. These data can be obtained free of charge from the Cambridge Crystallographic Data Center via www.ccdc.cam.ac.uk/data_request/cif.

Acknowledgments: D.T. is thankful to the Slovak National Scholarship Programme (2023) for a short research stay and Salale University, Addis Ababa Science and Technology University, Ethiopia, for a Ph.D studentship.

Conflicts of Interest: The authors declare no conflicts of interest.

References

1. Schiff, H. Mittheilungen Aus Dem Universitätslaboratorium in Pisa: Eine Neue Reihe Organischer Basen. *Justus Liebigs Ann. Chem.* **1864**, *131*, 118–119. [[CrossRef](#)]
2. Moutet, J.C.; Ourari, A. Electrocatalytic Epoxidation and Oxidation with Dioxygen Using Manganese(III) Schiff-Base Complexes. *Electrochim. Acta* **1997**, *42*, 2525–2531. [[CrossRef](#)]
3. Dixit, P.S.; Srinivasan, K. Effect of a Clay Support on the Catalytic Epoxidation Activity of a Manganese(III)-Schiff Base Complex. *Inorg. Chem.* **1988**, *27*, 4507–4509. [[CrossRef](#)]
4. Kessissoglou, D.P.; Butler, W.M.; Pecoraro, V.L. Characterization of Mono- and Binuclear Manganese(II) Schiff Base Complexes with Metal-Disulfide Ligation. *Inorg. Chem.* **1987**, *26*, 495–503. [[CrossRef](#)]
5. Itagaki, M.; Hagiya, K.; Kamitamari, M.; Masumoto, K.; Suenobu, K.; Yamamoto, Y. Highly Efficient Chiral Copper Schiff-Base Catalyst for Asymmetric Cyclopropanation of 2,5-Dimethyl-2,4-Hexadiene. *Tetrahedron* **2004**, *60*, 7835–7843. [[CrossRef](#)]
6. Sureshan, C.A.; Bhattacharya, P.K. Synthesis, Characterisation and Homogeneous Catalytic Activity Study of Mn(II) and Fe(III) Ternary Complexes. *J. Mol. Catal. A Chem.* **1998**, *136*, 285–291. [[CrossRef](#)]
7. Ramnauth, R.; Al-Juaid, S.; Motevalli, M.; Parkin, B.C.; Sullivan, A.C. Synthesis, Structure, and Catalytic Oxidation Chemistry from the First Oxo-Imido Schiff Base Metal Complexes. *Inorg. Chem.* **2004**, *43*, 4072–4079. [[CrossRef](#)]
8. Miyasaka, H.; Matsumoto, N.; Okawa, H.; Re, N.; Gallo, E.; Floriani, C. Complexes Derived from the Reaction of Manganese(III) Schiff Base Complexes and Hexacyanoferrate(III): Syntheses, Multidimensional Network Structures, and Magnetic Properties. *J. Am. Chem. Soc.* **1996**, *118*, 981–994. [[CrossRef](#)]
9. Gütllich, P.; Goodwin, H.A. Spin Crossover—An Overall Perspective. In *Spin Crossover in Transition Metal Compounds I. Topics in Current Chemistry*; Gütllich, P., Goodwin, H., Eds.; Springer: Berlin/Heidelberg, Germany, 2004; Volume 233. [[CrossRef](#)]
10. Takahashi, K.; Kawamukai, K.; Mochida, T.; Sakurai, T.; Ohta, H.; Yamamoto, T.; Einaga, Y.; Mori, H.; Shimura, Y.; Sakakibara, T.; et al. Antiferromagnetic Transition in a Novel Star-Shaped High-Spin Fe(III) Tetranuclear Cluster from a Mononuclear Coordination Anion Featuring π -Extended Schiff Base Ligands. *Chem. Lett.* **2015**, *44*, 840–842. [[CrossRef](#)]
11. Trávníček, Z.; Sindelár, Z. Crystal Structure of Ammonium Bis(2-Hydroxyphenyl-Salicylaldimine- O,N,O') Iron (III) Monohydrate. *Z. Kristallogr. NCS* **1997**, *212*, 125–126. [[CrossRef](#)]
12. Takahashi, K.; Kawamukai, K.; Okai, M.; Mochida, T.; Sakurai, T.; Ohta, H.; Yamamoto, T.; Einaga, Y.; Shiota, Y.; Yoshizawa, K. A New Family of Anionic Fe^{III} Spin Crossover Complexes Featuring a Weak-Field N₂O₄ Coordination Octahedron. *Chem. Eur. J.* **2016**, *22*, 1253–1257. [[CrossRef](#)] [[PubMed](#)]
13. Abdallah, S.M.; Mohamed, G.G.; Zayed, M.A.; El-Ela, M.S.A. Spectroscopic Study of Molecular Structures of Novel Schiff Base Derived from O-Phthaldehyde and 2-Aminophenol and Its Coordination Compounds Together with Their Biological Activity. *Spectrochim. Acta A Mol. Biomol. Spectrosc.* **2009**, *73*, 833–840. [[CrossRef](#)] [[PubMed](#)]
14. Jana, N.C.; Patra, M.; Brandão, P.; Panja, A. Synthesis, Structure and Diverse Coordination Chemistry of Cobalt(III) Complexes Derived from a Schiff Base Ligand and Their Biomimetic Catalytic Oxidation of o-Aminophenols. *Polyhedron* **2019**, *164*, 23–34. [[CrossRef](#)]
15. Tesfaye, D.; Linert, W.; Gebrezgiabher, M.; Bayeh, Y.; Elemo, F.; Sani, T.; Kalarikkal, N.; Thomas, M. Iron(II) Mediated Supramolecular Architectures with Schiff Bases and Their Spin-Crossover Properties. *Molecules* **2023**, *28*, 1012. [[CrossRef](#)] [[PubMed](#)]
16. Senthil Kumar, K.; Bayeh, Y.; Gebretsadik, T.; Elemo, F.; Gebrezgiabher, M.; Thomas, M.; Ruben, M. Spin-Crossover in Iron(II)-Schiff Base Complexes. *Dalton. Trans.* **2019**, *48*, 15321–15337. [[CrossRef](#)] [[PubMed](#)]
17. Bayeh, Y.; Osuský, P.; Yutronkie, N.J.; Gyepes, R.; Sergawie, A.; Hrobárik, P.; Clérac, R.; Thomas, M. Spin State of Two Mononuclear Iron(II) Complexes of a Tridentate Bis(Imino)Pyridine N-Donor Ligand: Experimental and Theoretical Investigations. *Polyhedron* **2022**, *227*, 30–32. [[CrossRef](#)]
18. Madhu, N.T.; Salitros, I.; Schramm, F.; Klyatskaya, S.; Fuhr, O.; Ruben, M. Above Room Temperature Spin Transition in a Series of Iron(II) Bis(Pyrazolyl)Pyridine Compounds. *Comptes Rendus Chim.* **2008**, *11*, 1166–1174. [[CrossRef](#)]

19. Bayeh, Y.; Suryadevara, N.; Schlittenhardt, S.; Gyepes, R.; Sergawie, A.; Hrobárik, P.; Linert, W.; Ruben, M.; Thomas, M. Investigations on the Spin States of Two Mononuclear Iron(II) Complexes Based on N-Donor Tridentate Schiff Base Ligands Derived from Pyridine-2,6-Dicarboxaldehyde. *Inorganics* **2022**, *10*, 98. [[CrossRef](#)]
20. Groom, C.R.; Bruno, I.J.; Lightfoot, M.P.; Ward, S.C. The Cambridge Structural Database. *Acta Cryst. Sect. B* **2016**, *72*, 171–179. [[CrossRef](#)]
21. Tunç, T.; Sarı, M.; Sadıkoğlu, M.; Büyükgüngör, O. Synthesis, Crystal Structure and Spectroscopic Studies of 2-((E)-[2-Hydroxyphenyl]imino)methyl Phenol Schiff Base Molecule. *J. Chem. Cryst.* **2009**, *39*, 672–676. [[CrossRef](#)]
22. Herchel, R.; Nemeč, I.; Machata, M.; Trávníček, Z. Experimental and Theoretical Investigations of Magnetic Exchange Pathways in Structurally Diverse Iron(III) Schiff-Base Complexes. *Inorg. Chem.* **2015**, *54*, 8625–8638. [[CrossRef](#)] [[PubMed](#)]
23. Dutta, A.K.; Biswas, S.; Dutta, S.; Dawe, L.N.; Lucas, C.R.; Adhikary, B. Syntheses, Structural, Spectroscopic and Magnetic Properties of Polynuclear Fe(III) Complexes Containing N and O Donor Ligands. *Inorg. Chim. Acta* **2016**, *444*, 141–149. [[CrossRef](#)]
24. Llunell, M.; Casanova, D.; Cirera, J.; Alemany, P.; Alvarez, S.; SHAPE. *Program for the Stereochemical Analysis of Molecular Fragments by Means of Continuous Shape Measures and Associated Tools*; Version 2.1; University of Barcelona: Barcelona, Spain, 2013; pp. 1–35.
25. Schünemann, V.; Winkler, H. Structure and Dynamics of Biomolecules Studied by Mossbauer Spectroscopy. *Rep. Prog. Phys.* **2000**, *63*, 263–353. [[CrossRef](#)]
26. Mørup, S. Magnetic Relaxation Phenomena. In *Mössbauer Spectroscopy and Transition Metal Chemistry*; Springer: Berlin/Heidelberg, Germany, 2011; pp. 209–234. [[CrossRef](#)]
27. Gunnlaugsson, H.P. Spreadsheet Based Analysis of Mössbauer Spectra. *Hyperfine Interact.* **2016**, *237*, 13–18. [[CrossRef](#)]
28. Oxford Diffraction. *CrysAlisPRO, (Version 1.171.41.93a)*; Oxford Diffraction Ltd.: Oxford, UK, 2020.
29. Sheldrick, G.M. SHELXT-Integrated Space-Group and Crystal-Structure Determination. *Acta Cryst. Sect. A Found. Crystallogr.* **2015**, *71*, 3–8. [[CrossRef](#)] [[PubMed](#)]
30. Sheldrick, G.M. Crystal structure refinement with SHELXL. *Acta Cryst. Sect. C Struct. Chem.* **2015**, *71*, 3–8. [[CrossRef](#)]
31. Farrugia, L.J. WinGX and ORTEP for Windows an update. *J. Appl. Cryst.* **2012**, *45*, 849–854. [[CrossRef](#)]
32. Brandenburg, K. *DIAMOND*; Crystal Impact GbR: Bonn, Germany, 2007.

Disclaimer/Publisher’s Note: The statements, opinions and data contained in all publications are solely those of the individual author(s) and contributor(s) and not of MDPI and/or the editor(s). MDPI and/or the editor(s) disclaim responsibility for any injury to people or property resulting from any ideas, methods, instructions or products referred to in the content.